



# Growth of InGaAs/InAlAs superlattices by MOCVD and precise thickness determination via HRXRD

Ilkay DEMIR, Sezai ELAGOZ<sup>1</sup> \*

<sup>1</sup>*Department of Nanotechnology Engineering, Nanophotonics Research and Application Center  
Cumhuriyet University, 58140, Sivas, Turkey*

Received: 09/06/2016    Revised: 10/07/2016    Accepted: 30/09/2016

---

## ABSTRACT

In this study, we report the growth studies of InGaAs/InAlAs superlattices (SLs) with thin layer thicknesses which will be used for quantum cascade laser (QCL) structures, grown by Metal Organic Chemical Vapor Deposition (MOCVD) technique. We utilize high resolution X-ray diffraction (HRXRD) to determine the single layer thickness and period thicknesses of SLs. Measurement results show that by establishing very low growth rates (~0,1 nm/s), the single thin layers and SLs can be grown well by MOCVD in a controllable and repeatable way with high crystalline and interface quality.

**Keywords:** *Superlattice, InGaAs, InAlAs, MOCVD, X-ray diffraction.*

---

## 1. INTRODUCTION

InGaAs and InAlAs semiconductor ternary compounds are crucial materials for electronic and optoelectronic devices such as Quantum Cascade Lasers (QCLs) [1-7], Quantum Well Infrared Photodetectors (QWIPs) [8-9], Field Effect Transistors (FETs) [10-11] and High Electron Mobility Transistors (HEMTs) [12-13] etc. InGaAs/InAlAs superlattices (SLs) are very attractive and suitable for QCL applications due to the availability of lattice matching and large conduction band offset. When  $\text{In}_x\text{Ga}_{1-x}\text{As}$  and  $\text{In}_y\text{Al}_{1-y}\text{As}$  compounds are lattice matched to InP substrate ( $x=0.53$ ,  $y=0.52$ ), the relative conduction band offset between them is ~520 meV [14]. At cryogenic temperatures, this allows emission at  $\lambda > 4\mu\text{m}$  [15]. Precise thickness control, alloy composition control and repeatability of the SLs are the most important issues to be dealt with in growth studies to obtain the desired complicated device structures. The

thinnest layer thickness is a few monolayers and the device performance is quite sensitive to interface roughness [16,17]. Molecular beam epitaxy (MBE) is generally preferred growth technique since it is more suitable for structures with very thin layers. However, the MOCVD could compete with MBE thanks to special growth conditions and continuously advancing mass flow controllers (MFCs) which control the gas quantity through the metalorganic sources and hydride sources. Additionally, MOCVD has a lot of extra parameters besides the source MFCs to precisely control the gas flow quantity of metalorganic sources such as bubbler pressure, bubbler temperature, dilution and injection tools.

Transmission Electron Microscope (TEM), Scanning Tunneling Electron Microscope (STEM) and similar

---

\*Corresponding author, e-mail: elagoz@cumhuriyet.edu.tr



We have three samples each with 50 periods of InGaAs/InAlAs, the only difference among them are their bilayer thickness (thus the growth time) selected in a clever way (same InGaAs thickness for different InAlAs thicknesses and the other way around) to compare the results. Table 1 shows the growth details of all samples.

**Table 1:** InGaAs and InAlAs growth times in a period of superlattice for sample A, B and C.

	InGaAs growth time (s)	InAlAs growth time (s)
Sample A	49.18	21.28
Sample B	49.18	35.46
Sample C	35.71	21.28

### 3. RESULTS AND DISCUSSION

We use in-situ reflectance measurements to observe the situation of surface, growth rate at real time and to measure the growth temperature of sample during growth. By using in-situ reflectance measurement it is very easy to determine the growth rate of samples with thick layers. However, for complicated device structures, such as the active region of a QCL structure, thickness determination of layers by in-situ reflectance is nearly impossible. For this reason, we use a detailed HRXRD analysis to determine the exact thicknesses and growth rates of alternately repeating thin layers. To insure that we get the correct values, we measured three superlattice structures (Sample A, B and C growth details given in experimental part) with similar parameters to compare and check the results. Fig.2 shows the 880 nm in-situ optical reflectance and temperature measurement during the growth of Sample A. In Fig.2, red curve shows the reactor temperature and the blue one represents the in-situ optical reflectance intensity. In situ optical reflectance and temperature measurements are divided into five parts as follows: (1) the increasing of the temperature up to 640 °C which is thermal deoxidization temperature and waiting at this temperature for 5 minutes in PH<sub>3</sub> ambient, (2) the growth of InP buffer layer, (3) preparation of precursor flows, (4) growth of InGaAs/InAlAs SLs and (5) cooling to room temperature in AsH<sub>3</sub> ambient. For each layer the starting point and the direction of reflectance curve can be different as seen in Inset of Fig. 2 which shows the InGaAs and InAlAs growth stages which give different optical reflectance behavior and direction due to the refractive index changing at each interface. The overall oscillation amplitude of the reflectance demonstrates that a high quality of growth takes places (no sudden or fast drops observed). The only drop in reflectance is a slow and uniform one caused by increasing absorption effects due to increasing of the film thickness.

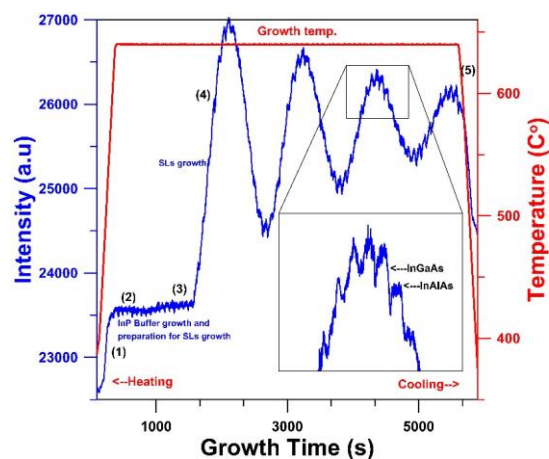


**Fig.2** In-situ optical reflectance measurement (blue curve) and temperature (red curve) during growth of sample A. Inset shows the InGaAs and InAlAs growth stages.

XRD is reliable, convenient, powerful and non-destructive technique to characterize the structural properties of single layers and SLs. HRXRD measurements were performed on each sample to obtain the effect of the variation in single layer thickness to the superlattice period.  $\omega$ -2 $\theta$  HRXRD measurement and simulation of sample A is shown in Fig.3. The highest and the narrowest peak in this measurement belongs to InP (400) peak of the substrate. There are five other peaks which belong to one period of SLs and we denoted as  $\Delta\theta$  which gives an angle difference between superlattice peaks. Also inset of Fig.3 shows another type of fringes that are more frequent and denoted with  $\delta\theta$  ( $<\Delta\theta$ ) which belongs to total thickness of SLs. For superlattice periodicity and total thickness calculation we used the equation shown below;

$$\frac{2 \sin\theta_n - 2 \sin\theta_{n+1}}{\lambda} = \pm \frac{n}{\Lambda}$$

where  $\Lambda$  is the SL period or if  $\delta\theta$  is used instead of  $\Delta\theta$  then  $\Lambda$  gives total thickness of the film,  $\lambda_{CuK\alpha} = 0.15405$  nm is the wavelength of incident X-ray,  $\theta_n$ ( $\theta_{n+1}$ ) is the Bragg angle of  $n^{\text{th}}$ ( $n+1^{\text{th}}$ ) order peak in  $\omega$ -2 $\theta$ . A careful analysis of the periodicity measurements from the  $\omega$ /2 $\theta$  scans gives the total thickness value of one period and even the total thickness of epitaxial structure (if the structure has high crystalline and interface quality) but not the individual layer thicknesses. Therefore, we have grown two samples (B and C) that are very similar in design to Sample A. The only one difference among these samples is the growth time (hence the thickness) of only one layer of the superlattice layers (InGaAs or InAlAs). From the equation, given above, we obtain 8.27 nm period thickness and 409 nm total thickness for sample A. Fig. 4 shows  $\omega$ -2 $\theta$  HRXRD measurement of sample B, its SLs peaks are spaced closer than sample A's because of the thicker period value. We have used same calculations for this sample to obtain 9.97 nm

period thickness and 459 nm total thickness. Fig. 5 shows  $\omega$ -2 $\theta$  HRXRD measurement of sample C, the angle differences between the nearest order SL peaks is the largest in sample C which means that it has the thinnest period thickness. For Sample C we obtained 6.67 nm period thickness and 348 nm total thickness. All the calculation results are briefly shown in Table 2.

**Table 2** Period thickness and total thickness of samples obtained from HRXRD measurements and calculations

	Period Thickness (nm)	Total Thickness (nm)
Sample A	8.27	409
Sample B	9.97	480
Sample C	6.67	348

The only difference between sample A and sample B is InAlAs growth time for each period. InAlAs growth time for sample A is 21.28 s while for the sample B it is 35.46 s. The time difference is 14.18 s and it gives a thickness difference of 1.70 nm for one period. It means that InAlAs layer has a growth rate of 0.119 nm/s-7.14  $\pm$  0.06 nm/min (1.70 nm/14.18 s). With the same approach for sample A InGaAs growth time is 49.18 s while for sample C it is 35.71 s for each period. The time difference is 13.47 s and it gives a thickness difference of 1.60 nm for one period. It means that InGaAs layer has a growth rate of 0,118 nm/s 7.08  $\pm$  0.06 nm/min (1.6 nm/13.47 s).

There is a small difference between bulk and superlattices in terms of growth rate. Superlattice growth rates less than the bulk ones. We believe that the reason of this difference comes from the growth environment one is being like homoepitaxy the other (SL) is like heteroepitaxy.

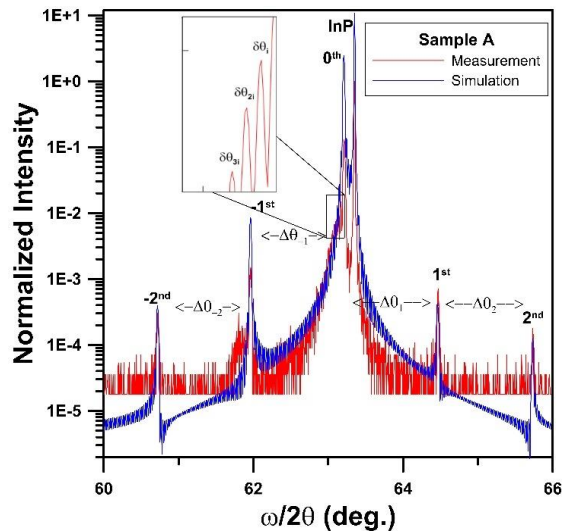


**Fig.3** HRXRD  $\omega$ /2 $\theta$  measurement (red) and simulation (blue) of sample A, inset shows fringes of total thickness of sample A

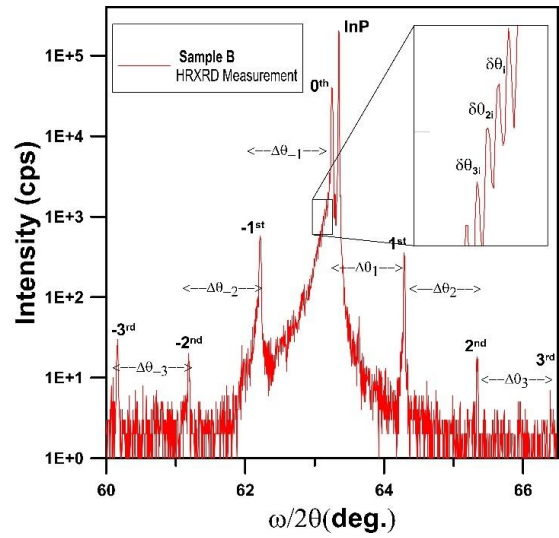


**Fig.4** HRXRD  $\omega$ /2 $\theta$  measurement of sample B, inset shows fringes of total thickness of sample.

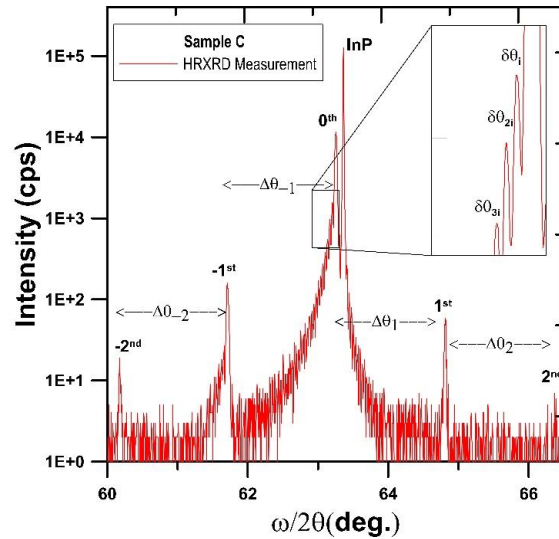


**Fig.5** HRXRD  $\omega$ /2 $\theta$  measurement of sample C, inset shows fringes of total thickness of sample.

**4. CONCLUSIONS**

Due to inability of using high precision in-situ measurement techniques in MOCVD growths, finding growth rates and individual layer thicknesses of SL structures with very thin layers is a major problem. In this study, it is shown that this difficulty can be handled by growing a series of samples with all growth parameters fixed except the growth time for a specific layer. Using these parametrically varied grown layers and using HRXRD measurements, it is possible to obtain the growth rates and the individual thin layer thicknesses precisely.

## ACKNOWLEDGEMENTS

This study was partially supported by Republic of Turkey, Ministry of Science, Industry and Technology-SANTEZ program under grant number 0573.STZ.2013-2. Ilkay Demir acknowledges the support through TUBITAK PhD Program fellowship BİDEB-2211 Grant

## CONFLICT OF INTEREST

No conflict of interest was declared by the authors.

## REFERENCES

- [1] M. Beck, D. Hofstetter, T. Aellen, J. Faist, U. Oesterle, M. Illegems, E. Gini, and H. Melchior. Continuous wave operation of a mid-infrared semiconductor laser at room temperature. *Science*, 295:5553–5557, 2002.
- [2] S. Blaser, D. A. Yarekha, L. Hvozdar, Y. Bonetti, A. Muller, M. Giovannini, and J. Faist. Above room temperature operation of short wavelength quantum cascade lasers at  $\lambda=5.4\mu\text{m}$ . *Appl. Phys. Lett.*, 86:041109, 2005
- [3] M. P. Semtsiv, M. Ziegler, S. Dressler, W. T. Masselink, N. Georgiev, T. Dekorsy, and M. Helm. Above room temperature operation of short wavelength ( $3.8 \mu\text{m}$ ) strain-compensated  $\text{In}_{0.73}\text{Ga}_{0.27}\text{As}-\text{AlAs}$  quantum cascade lasers. *Appl. Phys. Lett.*, 85:1478–1480, 2004.
- [4] Y. Bai, S. Slivken, S. Kuboya, S. R. Darvish, and M. Razeghi, "Quantum cascade lasers that emit more light than heat," *Nat Photon*, vol. 4, pp. 99-102, 02/print 2010.
- [5] R. Maulini, A. Lyakh, A. Tsekoun, and C. K. N. Patel, " $\lambda \sim 7.1 \mu\text{m}$  quantum cascade lasers with 19% wall-plug efficiency at room temperature," *Optics Express*, vol. 19, pp. 17203-17211, 2011/08/29 2011.
- [6] F. Xie, C. Caneau, H. P. Leblanc, D. P. Caffey, L. C. Hughes, T. Day, "Watt-Level Room Temperature Continuous-Wave Operation of Quantum Cascade Lasers With  $\lambda > 10 \mu\text{m}$ ," Selected Topics in Quantum Electronics, *IEEE Journal of*, vol. 19, pp. 1200407-1200407, 2013.
- [7] N. Bandyopadhyay, Y. Bai, B. Gokden, A. Myzaferi, S. Tsao, S. Slivken, M. Razeghi, "Watt level performance of quantum cascade lasers in room temperature continuous wave operation at  $\lambda \sim 3.76 \mu\text{m}$ ," *Applied Physics Letters*, vol. 97, pp. 131117-3, 09/27/ 2010.
- [8] X. Q. Lu · D. Y. Xiong · X. Tong, Photoresponse of  $\text{InGaAs/GaAs}$  multiple-period very-long-wavelength quantum well infrared photodetectors *Opt Quant Electron* (2015) 47:1429–1436
- [9] L. Guerra, G. M. Pene, L. D. Pintol, R. Jakomin, R. T. Moura, M. P. Pires, M. H. Degani, M. Z. Maialle and P. L. Souza, "InGaAs/InAlAs quantum well infrared photodetectors for operation in the 1.7 to 3.1  $\mu\text{m}$  wavelength range", *Microelectronics Technology and Devices (SBMicro)*, 2014 29th Symposium on, 1 – 310.1109/SBMicro.2014.6940111
- [10] Brian R. Bennett, Theresa F. Chick, J. Brad Boos, James G. Champlain, Adrian A. Podpirka, "Strained InGaAs/InAlAs quantum wells for complementary III–V transistors" *Journal of Crystal Growth* 388 (2014) 92–97.
- [11] Jung-Hui Tsai, Chia-Hong Huang, Jhih-Jhong Ou-Yang, Yi-Ting Chao, Jia-Cing Zhou, You-Ren Wu, "Performance and direct-coupled FET logic applications of InAlAs/InGaAs co-integrated field-effect transistors by 2-D simulation", *Thin Solid Films* 547 (2013) 267–271.
- [12] N. A. Yuzeeva, A. V. Sorokoumova, R. A. Lunin, L. N. Oveshnikov, G. B. Galiev, E. A. Klimov, D. V. Lavruchin, V. A. Kulbachinskii, "Electron Mobilities and Effective Masses in InGaAs/InAlAs HEMT Structures with High In Content" *J. Low Temp. Phys.*, DOI 10.1007/s10909-016-1589-6
- [13] Umesh P. Gomes, Yiqiao Chen, Sanjib Kabi, Peter Chow, Dhruv Biswas, "Quantum well engineering of InAlAs/InGaAs HEMTs for low impact ionization applications", *Current Applied Physics* 13 (2013) 487-492
- [14] I. Vurgaftman, J. R. Meyer, and L. R. Ram-Mohan, "Band parameters for III–V compound semiconductors and their alloys," *Journal of Applied Physics*, vol. 89, pp. 5815-5875, 06/01/ 2001.
- [15] Bandyopadhyay Neelanjan, Modelling, Design, Growth and Characterization of Strain Balanced Quantum Cascade Lasers (3-11 $\mu\text{m}$ ), grown by Gas Source Molecular Beam Epitaxy, Ph.D Northwestern University, 2015, Publication Number: AAT 3705212
- [16] S. G. Razavipour, E. Dupont, Z. R. Wasilewski, D. Ban" Effect of Interface Roughness Scattering on performance of Indirectly-Pumped Terahertz Quantum Cascade Lasers" *STh1F.3.pdf CLEO*, 2014
- [17] Ghasem Razavipour, Seyed; Dupont, Emmanuel; Wasilewski, Zbig R.; Ban, Dayan"Effects of interface roughness scattering on device performance of indirectly pumped terahertz quantum cascade lasers", *Journal of Physics: Conference Series*, Volume 619, Issue 1, article id. 012003 (2015).
- [18] W. C. H. Choy, P. J. Hughes, B. L. Weiss, E. H. Li, K. Hong and D. Pavlidis, The effect of growth interruption on the properties of InGaAs/InAlAs quantum well structures, *Appl. Phys. Lett.* 72 (1998) 338-340.
- [19] K. L. Fry, C. P. Kuo, R. M. Cohen, and G. B. Stringfellow, Photoluminescence of organometallic vapor phase epitaxial GaInAs, *Appl. Phys. Lett.*, 46 (1985) 955–957.